Naval Command,
Control and Ocean
Surveillance Center RDT&E Division San Diego, CA
92152-5001

Technical Report 1661
September 1994

Signal-to-Noise Gain From Adaptive Matched-Field Beamforming of Multidimensional Acoustic Arrays

Newell O. Booth
Gary L. Mohnkern

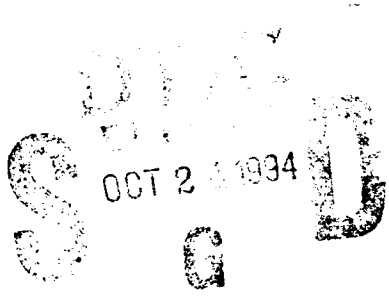

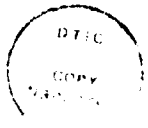

Technical Report 1661
September 1994

Signal-to-Noise Gain From Adaptive Matched-Field Beamforming of Multidimensional Acoustic Arrays

Newell O. Booth
Gary L. Mohnkern

NAVAL COMMAND, CONTROL AND
OCEAN SURVEILLANCE CENTER
RDT&E DIVISION
San Diego, California 92152–5001

K. E. EVANS, CAPT, USN
Commanding Officer

R. T. SHEARER
Executive Director

ADMINISTRATIVE INFORMATION

This work, conducted during FY 1990, was sponsored by the Office of Naval Research, High Gain Initiative, Program Element 602314, Project RJ14D35, Task 730-SW17.

Released by
Dr. C. D. Rees, Head
Acoustic Branch

Under authority of
Dr. J. H. Richter, Head
Ocean and Atmospheric
Sciences Division

SM

EXECUTIVE SUMMARY

OBJECTIVE

Estimate the array gain achievable using adaptive matched-field beamforming of large multi-dimensional acoustic arrays in coherent and incoherent noise fields.

APPROACH

A mathematical description of adaptive matched-field beamforming for coherent and incoherent noise fields is developed. Data covariance matrices are defined for 150 interference noise sources varying in level. The matched-field beamformer output and array gain are estimated when the array is focused on each of the sources for various interference-to-independent-noise ratios.

RESULTS

Array gain is predicted to be in excess of directivity index by the interference-to-independent-noise ratio and is observable for ratios of 0 dB and greater.

RECOMMENDATIONS

Experiments using multidimensional arrays of 100 to 1000 hydrophones are recommended to test the predictions.

CONTENTS

FIGURES

INTRODUCTION

Matched-field beamforming (MFB) is a generalization of plane-wave beamforming in which the complex steering vectors are modeled as solutions to the wave equation for the measured environment rather than as plane waves. Both linear, or Bartlett, and adaptive (e.g., minimum variance (MV)) processing schemes have been reported in the literature.[1,2,3,4,5,6] Beamformers provide signal-to-noise improvement (i.e., array gain) and estimates of signal parameters. In contrast to plane wave beamforming of a volumetric array, which estimates the azimuth and elevation of the signal arrival, MFB estimates the range, depth, and azimuth of the source of signals incident on the array.

This report reviews linear and adaptive matched-field beamforming processors and derives expressions for the mean array gain of the processors, assuming either incoherent or correlated noise. The energy contribution of an interference on a sidelobe is calculated to provide peak sidelobe criteria for array design. The sensitivity to mismatch of the processors is examined versus the number of hydrophones and the input-signal-to-noise ratio.

MATCHED-FIELD BEAMFORMERS

Consider a multidimensional array with horizontal and vertical aperture sufficient to resolve interferences and element spacing larger than $\lambda/2$ in an arbitrary ocean environment similar to that shown in figure 1. The acoustic array data contain samples of the signal and noise incident upon the array. The hydrophone data are conditioned, filtered, sampled, and Fourier analyzed, generating a complex Fourier coefficient for each frequency, hydrophone, and time sample. The data for each frequency bin are organized into a data matrix:

$$\mathbf{X} = \begin{matrix} \\ e \\ l \\ e \\ m \\ e \\ n \\ t \\ s \end{matrix} \begin{matrix} \overset{time\ samples}{} \\ \begin{bmatrix} x_{11} & x_{12} & \cdot & \cdot & \cdot & x_{1T} \\ x_{21} & x_{22} & \cdot & \cdot & \cdot & x_{2T} \\ \cdot & \cdot & \cdot & \cdot & \cdot & \cdot \\ \cdot & \cdot & \cdot & \cdot & \cdot & \cdot \\ x_{N2} & x_{N2} & \cdot & \cdot & \cdot & x_{NT} \end{bmatrix} \end{matrix} \tag{1}$$

where N is the number of array hydrophones and T is the number of time samples. A covariance matrix is estimated by averaging over the time that targets are in a search cell ($^+$ denotes complex transpose):

$$\hat{\mathbf{K}} = \mathbf{X}\mathbf{X}^+ \tag{2}$$

The signal energy arriving during the averaging time in a search cell is estimated using either linear or adaptive matched-field beamforming.

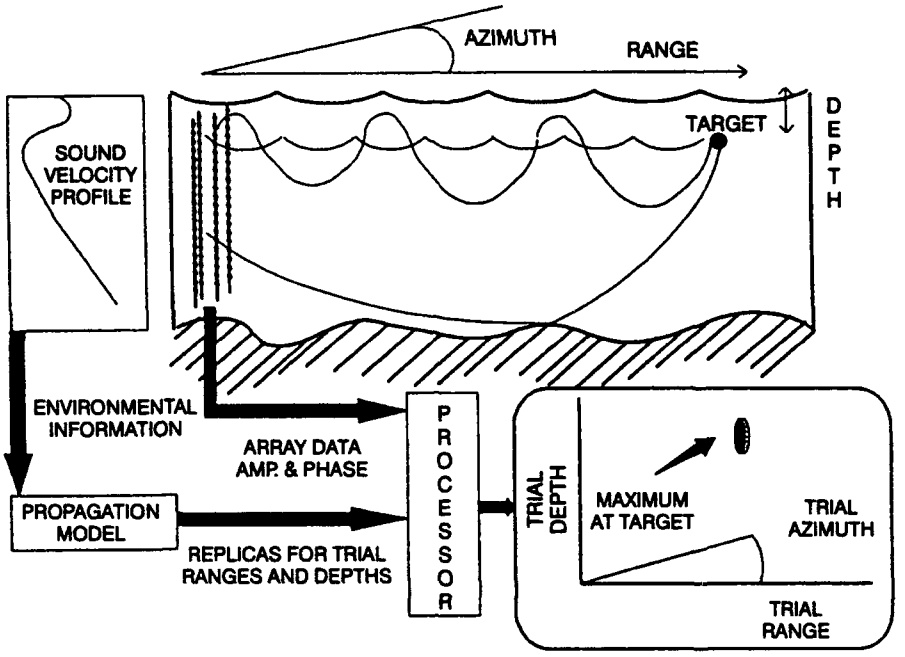

Figure 1. Matched-field beamforming process.

LINEAR MATCHED-FIELD BEAMFORMING

Linear beamforming in the frequency domain estimates the received energy by applying steering vectors to the estimated covariance:

$$\langle E_L(\hat{a}) \rangle = \mathbf{s}^+(\hat{a})\ \hat{\mathbf{K}}\ \mathbf{s}(\hat{a}) \tag{3}$$

where $\mathbf{s}^+(\hat{a})$ is the complex steering vector. The energy is estimated for each search cell in the search area by varying the trial parameter, $\hat{a}$, of the steering vector and searching for an energy peak. The position of the peak is an estimate of the range, depth, and azimuth of the signal source. $\mathbf{s}(\hat{a})$ is calculated by using measurements of the array element locations, estimates of the sound speed structure derived from oceanographic measurements, and acoustic propagation models.

In the far-field plane-wave beamforming case, the signal model assumes a plane wave parameterized in azimuth and elevation, $\hat{a} = (\theta, \phi)$. For focused beamforming, the signal model is a spherical wave propagating from a target location parameterized in range, azimuth, and elevation, $\hat{a} = (r, \theta, \phi)$. In both cases, the complex steering weight is of the form $s_j = e^{-j\Phi j}$ with unit amplitude and is normalized according to

$$\sum_{j=1}^{N} s_j s_j^* = N \tag{4}$$

For matched-field beamforming, the signal is modeled with an acoustic propagation model parameterized in trial range, depth, and azimuth. $\hat{a} = \vec{r} \equiv (r, d, \theta)$ is the set of search space

parameters. The vector $\mathbf{s} = (s_1, s_2, \ldots s_N)$ is called the replica for a signal at the trial location. Using the normalization from Eq. 4, the steering vector is derived from the modelled pressures by

$$s_j(\hat{a}) = \frac{p_j(\hat{a})}{\sqrt{\frac{\sum_{k=1}^{N} p_k(\hat{a})\, p_k^*(\hat{a})}{N}}} \tag{5}$$

The replica accounts for the propagation multipaths and curved wavefronts included in the propagation model. The replica amplitude and phase both depend on the hydrophone, *j*, because of the depth dependence of the propagation and vertical multipath interference pattern. Plane-wave and focused beamforming are special cases of matched-field beamforming which assume plane- and spherical-wave propagation models.

ADAPTIVE MATCHED-FIELD BEAMFORMING

In adaptive MFB, the output energy is estimated according to

$$\langle E_A(\hat{a}) \rangle = \mathbf{w}^+(\hat{a})\ \hat{\mathbf{K}}\ \mathbf{w}(\hat{a}) \tag{6}$$

The adaptive weights are determined from the estimated covariance, $\hat{\mathbf{K}}$, to minimize the output energy subject to the constraint

$$\mathbf{w}^+(\hat{a})\ \mathbf{s}(\hat{a}) = \sum_{j=1}^{N} w_j^*(\hat{a})\ s_j(\hat{a}) = 1 \tag{7}$$

Adaptive MFB minimizes the energy received by nulling interferences, while the constraint assures that signals matching the replica vector, **s**, are passed without distortion. The minimum variance weight vector is given by

$$\mathbf{w}_A(\hat{a}) = \frac{\hat{\mathbf{K}}^{-1}\mathbf{s}(\hat{a})}{\mathbf{s}^+(\hat{a})\hat{\mathbf{K}}^{-1}\mathbf{s}(\hat{a})} \tag{8}$$

and the output energy is obtained by substituting in Eq. 6:

$$\langle E_A(\hat{a}) \rangle = \frac{1}{\mathbf{s}^+(\hat{a})\ \hat{\mathbf{K}}^{-1}\ \mathbf{s}(\hat{a})} \tag{9}$$

Minimizing energy is accomplished in the process by using the measured data to estimate the amplitudes and phases of interference signals which do not match the steering vector and coherently subtracting the energy. Knowledge of the replica vectors for the interferences, including the associated locations and propagation parameters, is not required by the process. Knowledge of the interference positions can be used in the inverse problem to estimate the sound-speed structure and array element positions.[7]

SUMMARY

Matched-field beamforming allows the use of large vertical apertures which fill the water column. It provides the potential of separating submerged target signals from surface and sound channel noise. If plane-wave beamforming were to be performed on the array, its vertical resolution would be ~1 degree. Arrival angles from nonbottom interacting sources typically vary between ±20 degrees. The plane-wave beamformer smears the signal multipath arrivals, resulting in gain degradation. MFB combines the coherent vertical signal multipath and corrects for changes of signal arrival angle over the vertical aperture.

Adaptive MFB reduces sidelobe energy by minimizing the energy that does not match the signal replica constraint. By focusing on the signal source and minimizing the sidelobe energy, the processor increases the signal-to-noise ratio (SNR).

ARRAY GAIN IN NONUNIFORM INCOHERENT NOISE

For the purposes of this section, it is assumed that the ocean has a single point source with incoherent noise which varies from element to element. **K** then has the form

$$\mathbf{K} = \sigma_s^2 \mathbf{d}\mathbf{d}^+ + \sigma_n^2 \Lambda \tag{10}$$

where $\mathbf{d}\mathbf{d}^+$ is the dyadic matrix formed from the vector of pressures from a source at the source position $\vec{r}_s = (r_s, d_s, \theta_s)$. The average signal energy incident on the array is σ_s^2. Λ is a diagonal matrix of the relative noise energy and σ_n^2 is the average noise in the array elements. If the noise energy is equal on all of the hydrophones, $\Lambda = \mathbf{I}$, the identity matrix.

LINEAR MFB IN INCOHERENT NOISE

For a linear beamformer, the output energy from Eq. 3 is given by

$$\langle E_L(\hat{a}, \vec{r}_s) \rangle = \sigma_s^2 \ \mathbf{s}^+(\hat{a})\mathbf{d}(\vec{r}_s)\mathbf{d}^+(\vec{r}_s)\mathbf{s}(\hat{a}) + \sigma_n^2 \mathbf{s}^+(\hat{a})\Lambda\mathbf{s}(\hat{a}) \tag{11}$$

Assuming perfect match, $\mathbf{s} = \mathbf{d}$, and using Eq. 4, the output energy becomes

$$\langle E_L(\hat{a}, \vec{r}_s) \rangle = N^2\sigma_s^2 + N \ \overline{\lambda_n}^s \sigma_n^2 \tag{12}$$

where

$$\overline{\lambda_n}^s = \frac{\mathbf{s}^+ \Lambda \mathbf{s}}{N} = \frac{\sum_{j=1}^{N} s_j s_j^* \lambda_j}{N} \tag{13}$$

is the signal weighted average relative noise power in the array elements, which accounts for the combination of noise and signal variation across the array. For example, if the noise is high on the elements where the signal energy is high, then $\overline{\lambda_n}^s$ will be higher and the gain will be lower. Note that if either the noise is equal on all elements or all the signal powers are equal (as in plane-wave beamforming), then $\overline{\lambda_n}^s = 1$.

From Eq. 12, we see that when the matched-field beamformer is steered at the signal, the signal energy increases by N^2 and the noise energy increases by N. The array gain is defined as the output SNR divided by the input SNR:

$$AG = 10 \log \frac{\left(\frac{\langle E(\sigma_n^2 = 0) \rangle}{\langle E(\sigma_s^2 = 0) \rangle} \right)}{\left(\frac{\sigma_s^2}{\sigma_n^2} \right)} \tag{14}$$

For linear MFB, the array gain is given by

$$AG_L = 10 \log \left(\frac{N}{\overline{\lambda_n^{-1}}^s} \right) \tag{15}$$

The array gain in uniform incoherent noise, $\Lambda = \mathbf{I}$, is the directivity index, $DI = 10 \log N$.

ADAPTIVE MFB IN INCOHERENT NOISE

For adaptive MFB, the output energy from Eq. 9 is given by

$$\langle E_A(\hat{a}, \vec{r}_s) \rangle = \frac{1}{\mathbf{s}^+(\hat{a}) \left(\sigma_s^2 \ \mathbf{d}(\vec{r}_s)\mathbf{d}^+(\vec{r}_s) \ + \ \sigma_n^2 \Lambda \right)^{-1} \mathbf{s}(\hat{a})} \tag{16}$$

Assuming perfect match ($\mathbf{s} = \mathbf{d}$), and using[8]

$$\left[\mathbf{USV}^+ + \mathbf{B} \right]^{-1} = \mathbf{B}^{-1} - \mathbf{B}^{-1}\mathbf{U} \left[\mathbf{V}^+\mathbf{B}^{-1}\mathbf{U} + \mathbf{S}^{-1} \right]^{-1} \mathbf{V}^+\mathbf{B}^{-1} \tag{17}$$

the output energy and optimum weight vector become

$$\langle E_A(\hat{a}, \vec{r}_s) \rangle = \sigma_s^2 + \frac{\sigma_n^2}{N \overline{\lambda_n^{-1}}^s} \tag{18}$$

$$\mathbf{w_A} = \frac{\Lambda^{-1}\mathbf{s}}{\mathbf{s}^+\Lambda^{-1}\mathbf{s}} \tag{19}$$

where $\overline{\lambda_n^{-1}}^s = \frac{\mathbf{s}^+\Lambda^{-1}\mathbf{s}}{N} = \frac{\sum_{j=1}^{N} \frac{s_j s_j^*}{\lambda_j}}{N}$ is the mean of the inverses of the relative noise power in the array elements weighted by the relative signal powers. The array gain becomes

$$AG_A = 10 \log \left(N \overline{\lambda_n^{-1}}^s \right) \tag{20}$$

If the noise is equal on all elements, $\overline{\lambda_n^{-1}}^s = 1$, adaptive MFB has the same weights and array gain as linear MFB. When the noise varies from element to element, the elements with high

noise are weighted less than the elements with low noise. Thus, even in the case with incoherent but unequal noise, the array gain is increased with adaptive processing.

ARRAY GAIN IN NOISE WITH MULTIPLE UNCORRELATED INTERFERENCES

In this section, the array gain is derived by assuming that the array noise consists of signals from M uncorrelated sources plus uniform independent element noise. The source, labeled k, is defined as the signal upon which the array is focused. The covariance matrix for this assumption is

$$\mathbf{K} = \sigma_k^2 \mathbf{d}_k \mathbf{d}_k^+ + \mathbf{K}_n$$
$$\mathbf{K}_n = \sum_{\substack{j=1 \\ j \neq k}}^{M} \sigma_j^2 \mathbf{d}_j \mathbf{d}_j^+ + \sigma_n^2 \mathbf{I} \tag{21}$$

It is also assumed that the independent noise is equal on all elements. The effects of unequal but independent noise are similar to that discussed in the preceding section.

LINEAR MFB WITH MULTIPLE INTERFERENCES

Assuming that the array is steered at the signal $\mathbf{s} = \mathbf{d}_k$, the energy at the output of a linear matched-field beamformer (using Eq. 3, 4, and 21) is given by

$$\langle E_L \rangle = N^2 \sigma_k^2 + N^2 \sum_{\substack{j=1 \\ j \neq k}}^{M} \sigma_j^2 L_{js} + N\sigma_n^2 \tag{22}$$

where $\mathbf{s}^+ \mathbf{d}_j \mathbf{d}_j^+ \mathbf{s} = N^2 L_{js}$ and L_{js} is the sidelobe power level for a linear beamformer of the j^{th} signal when the array is steered at $\mathbf{s}$.

For this case, the array gain is defined as the output-signal-to-total-noise ratio divided by the input-signal-to-total noise-ratio

$$AG = 10 \log \frac{\left(\frac{\langle E(\sigma_n^2 = \sigma_j^2 = 0) \rangle}{\langle E(\sigma_k^2 = 0) \rangle} \right)}{\left(\frac{\sigma_k^2}{\sigma_T^2} \right)} \tag{23}$$

where $\sigma_T^2 = \sigma_n^2 + \sum_{\substack{j=1 \\ j \neq k}}^{M} \sigma_j^2$ is the total noise energy. The linear array gain is given by

$$AG_L = 10 \log N - 10 \log \left[\frac{1 + N \sum_j \alpha_j^2 L_{js}}{1 + \alpha_I^2} \right] \tag{24}$$

where $\alpha_j^2 = \sigma_j^2/\sigma_n^2$ is the input interference-to-independent-noise ratio (IINR) for the j^{th} interference and $10\log\alpha_j^2 = 10\log\left[\sum_{\substack{j=1 \\ j=/k}} \alpha_j^2\right]$ is the total IINR, $IINR_T$.

Note that array gain is reduced from the isotropic noise case by the interference signals in the sidelobes. If there is no interference in the main beam and all the sidelobes are lower than $1/N$, gain better than $10 \log N$ can be achieved for all resolved signals. When the array is steered where an interference is in a high sidelobe, the gain is less than $10 \log N$. Obtaining low sidelobes requires a large number of elements, closely spaced and with high tolerance on the amplitude and phase. Linear MFB gain, even with most careful array design, will typically be less than $10 \log N$ because sidelobes within a few decibels of the main lobe occur at convergence zone (CZ) spacing.[2] These sidelobes result from propagation in the oceanic waveguide and cannot be reduced by array design methods.

In the discussion of linear mismatch effects, Eq. 42, it is shown that the mean sidelobe level is $\overline{L_s} = \frac{1}{N}$. The linear MFB array gain in coherent noise, assuming all interferences are at the mean sidelobe level, reduces to the directivity index, $\overline{AG_L} = 10 \log N = DI$.

ADAPTIVE MFB WITH MULTIPLE INTERFERENCES

Adaptive MFB reduces the sidelobe energy whenever the sidelobe is greater than a few decibels down from the main lobe. This helps in removing the CZ sidelobes and allows the use of thinned arrays with element spacing greater than $\lambda/2$.[9]

Using Eq. 17, it can be shown that if $\mathbf{K} = a\,\mathbf{d}\mathbf{d}^+ + \mathbf{K}_n$, then

$$\mathbf{K}^{-1} = \mathbf{K}_n^{-1} - a\,\mathbf{K}_n^{-1}\mathbf{d}\;[1 + a\,\mathbf{d}^+\mathbf{K}_n^{-1}\mathbf{d}]^{-1}\mathbf{d}^+\mathbf{K}_n^{-1} \tag{25}$$

The output energy of adaptive MFB becomes

$$\langle E_A \rangle = \frac{1 + \sigma_k^2 \mathbf{d}_k^+ \mathbf{K}_n^{-1}\mathbf{d}_k}{\mathbf{s}^+\mathbf{K}_n^{-1}\mathbf{s}\left[1 + \sigma_k^2 \mathbf{d}_k^+ \mathbf{K}_n^{-1}\mathbf{d}_k \left(1 - \frac{\mathbf{s}^+\mathbf{K}_n^{-1}\mathbf{d}_k\;\mathbf{d}_k^+\mathbf{K}_n^{-1}\mathbf{s}}{\mathbf{s}^+\mathbf{K}_n^{-1}\mathbf{s}\;\mathbf{d}_k^+\mathbf{K}_n^{-1}\mathbf{d}_k}\right)\right]} \tag{26}$$

When the steering vector matches the signal vector ($\mathbf{s} = \mathbf{d}_k$) the term in (..) equals zero, giving the following equation for the output energy:

$$\langle E_A \rangle = \sigma_k^2 + \frac{1}{\mathbf{s}^+\mathbf{K}_n^{-1}\mathbf{s}} \tag{27}$$

From repeated applications of Eq. 17 to in Eq. 21 (see Appendix), the following expression can be derived for the inverse of the total noise covariance matrix:

$$\mathbf{K}_n^{-1} = \frac{1}{\sigma_n^2}\left[\mathbf{I} - \sum_{\substack{j=1 \\ j \neq k}}^{M}\left(\frac{\sigma_j^2 \mathbf{d}_j \mathbf{d}_j^+}{\sigma_n^2 + N\sigma_j^2}\right)\right] \tag{28}$$

The output energy of the adaptive MFB process is given by

$$\langle E_A \rangle = \sigma_k^2 + \frac{\sigma_n^2}{N} \left[\frac{1}{1 - N \sum_{\substack{j=1 \\ j \neq k}}^{M} \left(\frac{\alpha_j^2 L_{js}}{1 + N\alpha_j^2} \right)} \right] \tag{29}$$

and the array gain is given by

$$AG_A = 10 \log \left[N(1 + \alpha_I^2) \left[1 - N \sum_{\substack{j=1 \\ j \neq k}}^{M} \left[\frac{\alpha_j^2 L_{js}}{1 + N\alpha_j^2} \right] \right] \right] \tag{30}$$

Using $\overline{L_s} = \frac{1}{N}$ (Eq. 42), the adaptive MFB output energy, assuming all interferences are at the mean sidelobe level, is given by

$$\langle E_A \rangle = \sigma_k^2 + \frac{\sigma_n^2}{N} \left[\frac{1}{1 - \sum_{\substack{j=1 \\ j \neq k}}^{M} \left(\frac{\alpha_j^2}{1 + N\alpha_j^2} \right)} \right] \tag{31}$$

and the array gain is given by

$$AG_A = 10 \log \left[N(1 + \alpha_I^2) \left[1 - \sum_{\substack{j=1 \\ j \neq k}}^{M} \left[\frac{\alpha_j^2}{1 + N\alpha_j^2} \right] \right] \right] \tag{32}$$

As the number of elements increases, $N>M$, the array gain increases asymptotically as

$$AG_A \underset{N \gg M}{\rightarrow} 10 \log N + 10 \log \alpha_I^2 \tag{33}$$

The array gain is then bounded by 10 log N plus $IINR_T$.

The array gain and output energy from adaptive MFB can be calculated for various α_i^2 by using Eq. 31 and 32, and by assuming a distribution of interference levels, σ_j^2. We assume, in figure 2, that the acoustic field consists of 150 sources of varying levels, with a total level of 79.95 dB. In this example, the total noise level is 80 dB. The total input interference to independent noise, $IINR_T$, is assumed to be 10 dB.

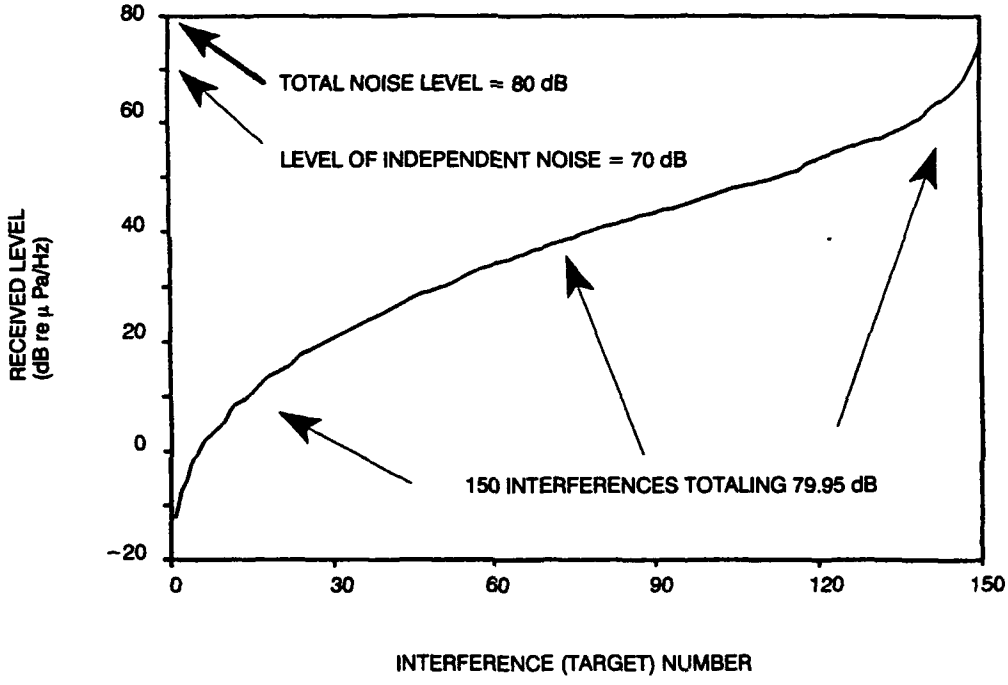

Figure 2. Noise field assumption for figure 3. Total noise level = 80 dB. Independent noise level = 69.95 dB. 150 interferences uniformly distributed in energy, totaling 79.95 dB.

The received energy when the array is focused at each of the interferences is shown in figure 3 for various number of array elements, N. As N increases, the measured noise floor drops and more signals are detected. For example, with 1,000 hydrophones, signals approximately 40 dB below the 80-dB total noise level can be detected, achieving a 40-dB array gain, 10 dB above 10 log N.

The array gain in this noise field, calculated by using Eq. 32, is shown in figure 4 versus N. In this plot, $IINR_T$ is varied from -30 to +20 dB. The conditions of figure 2 and figure 3, $IINR_T$ = 10 dB, are marked with "+" in the figure. From figure 4, measurements with 1,000-element volumetric arrays can determine the IINR. The array gain achievable with a larger number of elements is 10 log N + $IINR_T$.

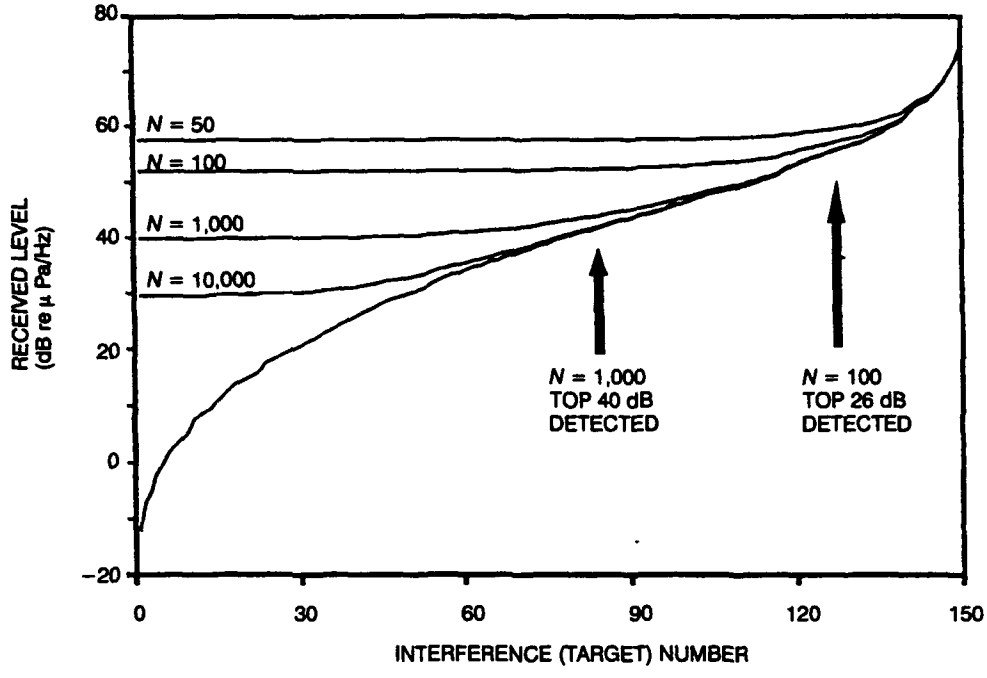

Figure 3. Received level from adaptive MFB versus number of elements, N, when the processor is steered at the interference.

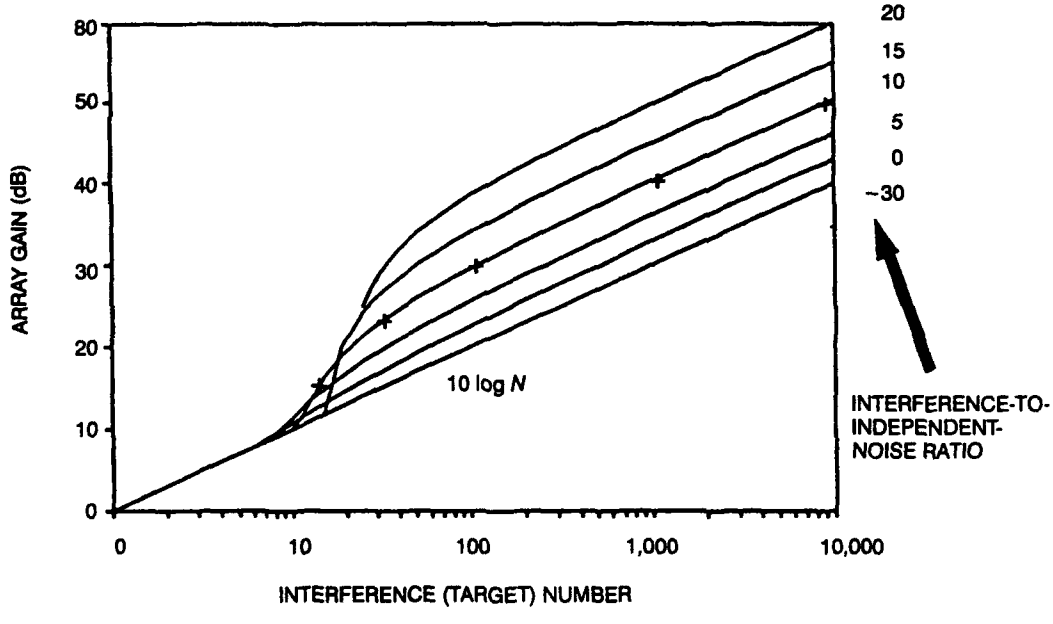

Figure 4. Array gain vs number of elements, N, and total-interference-to-independent-noise ratio, $IIINR_T$.

PEAK SIDELOBE LEVEL REQUIREMENTS FOR ADAPTIVE MFB

The results presented above are expected values since the mean sidelobe level of $-10 \log N$ was used. In order to establish array design criteria, the portion of the noise floor energy of a given interference is estimated by assuming one signal (k), one interference (i), and independent noise in Eq. 29. This is given by

$$\langle E_A \rangle (\mathbf{s}_k \neq \mathbf{d}_i) = \sigma_k^2 + \frac{\sigma_n^2}{N} \left[\frac{1}{1 - \frac{N\alpha_i^2 L_{is}}{1 + N\alpha_i^2}} \right] \tag{34}$$

The second term is the contribution to the noise floor from the interference. It is plotted in figure 5 versus the sidelobe level (L_{is}) as a function of N and the individual interference-to-independent-noise ratio, $IINR_i = 10 \log \alpha_i^2$. For large $IINR_i$, an interference contributes 1 dB to the noise floor for peak sidelobes below –6 dB re the main lobe. A few sidelobes as high as –3 dB are acceptable. Arrays can be designed by using the linear matched-field beampattern statistics in a process similar to random arrays.[9,10,11,12]

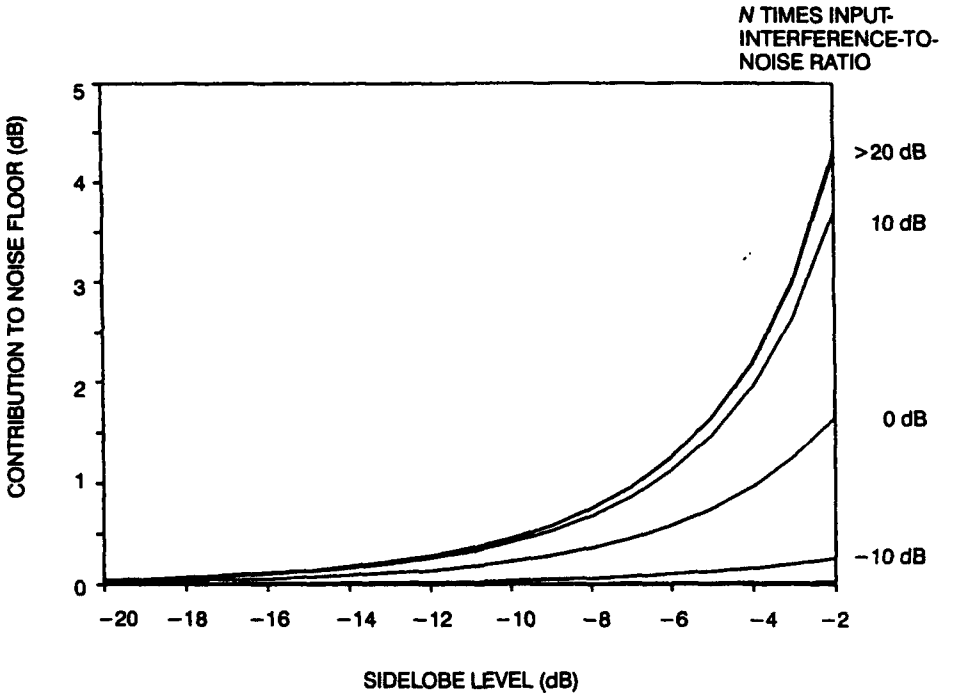

Figure 5. Contribution to the measured noise floor from a single interference versus the Bartlett sidelobe level at the interference for vaious $N \times IINR_i$.

The high sidelobe tolerance of adaptive MFB has great impact on the design of arrays, eliminating the need for large numbers of accurately positioned high-tolerance hydrophone channels, which are required to obtain the low sidelobe levels needed to detect weak signals in multiple interferences.

SENSITIVITY OF MATCHED-FIELD BEAMFORMING TO MISMATCH ERRORS

Errors in element location, propagation modeling, and sound-speed structure measurement result in errors in the prediction of the signal replica, **s**. These mismatch errors cause both loss of array gain and bias errors in estimating the source position.[2] The latter occur when a near perfect match is obtained for true source positions that differ from the estimated positions, $\vec{r}_s \neq \hat{a}$. The sensitivity of array gain and output spectrum of optimum array processors has been thoroughly analyzed by Cox.[13] Though derived assuming plane wave propagation, his results are directly applicable to matched-field beamformers. For this report, we examine the array spectral output degradation (ASOD) due to mismatch, defined as the ratio of the energy at the signal peak with mismatch to the energy with no mismatch:

$$ASOD = 10 \log\left(\frac{\langle E\rangle_{MM}}{\langle E\rangle}\right) \tag{35}$$

This definition is experimentally estimated using a strong signal at a known position. The energy in the peak nearest the known location is measured and compared to the predicted energy with no mismatch. The definition and measurement include a component of the output energy from increased sidelobes caused by the nulling of the mismatched signal. This section describes the array gain degradation (AGD) for linear and adaptive MFB as a function of input SNR. It is assumed that the acoustic field is generated by a single-point source and incoherent noise. The covariance matrix is shown in Eq. 10.

LINEAR MFB MISMATCH EFFECTS

In practice, the signal energy measurement includes some noise energy, as shown in Eq. 12. Linear array spectral output degradation, $ASOD_L$, is obtained using Eq. 11 and 12 in Eq. 35:

$$\begin{aligned} ASOD_L &= 10 \log\left[\frac{\sigma_s^2(\mathbf{s}^+\mathbf{d}\,\mathbf{d}^+\mathbf{s}) + N\overline{\lambda_n}^s\sigma_n^2}{N^2\sigma_s^2 + N\overline{\lambda_n}^s\sigma_n^2)}\right] \\ &= 10 \log\left[\frac{\cos^2(\mathbf{s},\mathbf{d}) + \frac{\overline{\lambda_n}^s}{N\alpha^2}}{1 + \frac{\overline{\lambda_n}^s}{N\alpha^2}}\right] \end{aligned} \tag{36}$$

where $\alpha^2 = \left(\frac{\sigma_s^2}{\sigma_n^2}\right)$ is the input SNR and

$$\cos^2(\mathbf{s}, \mathbf{d}) = \frac{(\mathbf{s}^+\mathbf{d})(\mathbf{d}^+\mathbf{s})}{(\mathbf{s}^+\mathbf{s})(\mathbf{d}^+\mathbf{d})} \tag{37}$$

is the generalized cosine between the steering vector, **s**, and the signal vector, **d**.[13] The latter is a measure of the mismatch signal gain degradation which results from nonalignment between the steering vector and the received signal vector. It is also the ASOD and AGD for a large output

SNR. The linear ASOD for various output SNRs, $N\alpha^2$, is plotted in figure 6 as a function of mismatch AGD, 10 log $\cos^2(\mathbf{s}, \mathbf{d})$. We have assumed equal noise on all of the elements, $\overline{\lambda_n}^s = 1$. Note that the output SNR must be 20 dB or greater for a direct measurement of ASOD. However, a measurement of the input SNR, $\overline{\lambda_n}^s$, and ASOD can be used with Eq. 36 to estimate the mismatch AGD with finite SNR.

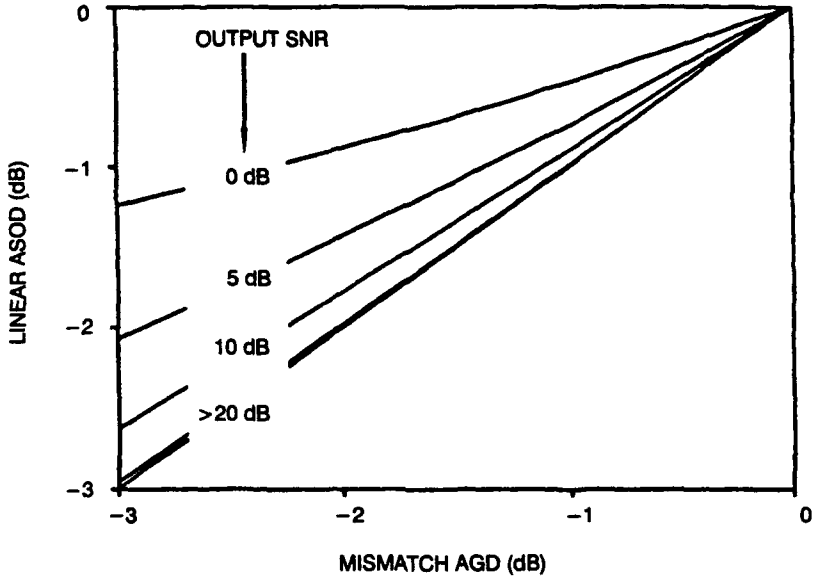

Figure 6. Bartlett array gain degradation versus mismatch array gain degradation for various output SNRs.

Following the work of Berman,[14] we assume that **s** and **d** differ only in phase, $d_j = s_j e^{-i\delta_j}$. The true mismatch is given by

$$\cos^2(\mathbf{s}, \mathbf{d}) = \frac{\left[\sum_{j=1}^{N} s_j^2 e^{-i\delta_j}\right]\left[\sum_{k=1}^{N} s_k^2 e^{i\delta_k}\right]}{N^2} = \frac{\sum_{j=1}^{N} s_j^4 + \sum_{j=1}^{N}\sum_{k=1, k\neq j}^{N} s_j^2 s_k^2 e^{-i(\delta_j - \delta_k)}}{N^2} \tag{38}$$

If it is assumed that the mismatch errors are represented by independent Gaussian distributed phase errors on each element of the array, given by

$$P(\delta_k = \frac{1}{\sqrt{2\pi\delta^2}} e^{-\frac{\delta_k^2}{2\delta^2}} \tag{39}$$

where $\overline{\delta^2}$ is the RMS phase error in radians; then

$$\langle e^{-i(\delta_j - \delta_k)} \rangle = e^{-\overline{\delta^2}} \tag{40}$$

We have used the fact that the probability density of the difference of two independent zero mean normal distributions is also a zero mean normal distribution whose variance is the sum of the component variances.

Using $\left(\sum_{j=1}^{N} s_j^2 \right)^2 = \sum_{j=1}^{N} s_j^4 + \sum_{j=1}^{N} \sum_{j \neq k}^{N} s_j^2 s_k^2$ and Eq. 4 in Eq. 38, the expected value of the output with mismatch is given by

$$\langle \cos^2(\mathbf{s}, \mathbf{d}) \rangle = \frac{1 + (N_e - 1) e^{-\overline{\delta^2}}}{N_e} \tag{41}$$

where $N_e = \frac{N^2}{\sum_{j=1}^{N} s_j^4}$ is the effective number of elements illuminated by the signal.

The mismatch AGD from phase errors is plotted in figure 7. It can be seen that the signal replica at a range near the true range must be calculated to $\frac{\lambda}{10}$ relative accuracy. This implies that relative array element locations be known to better than $\frac{\lambda}{10}$ and that the acoustic models and sound-speed structure measurements generate replicas to this relative accuracy.

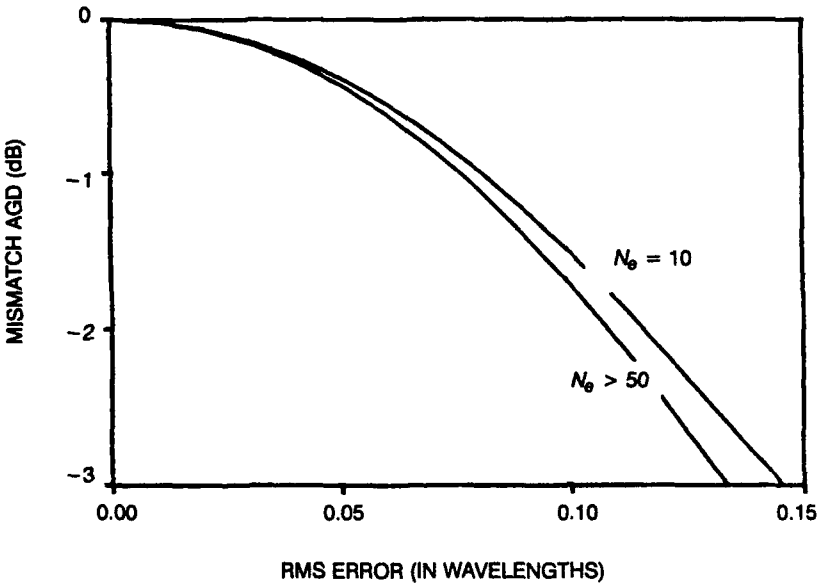

Figure 7. Expected mismatch array gain degradation versus RMS phase error in wavelengths.

Equation 41 can also be used to derive an expression for the mean sidelobe level. Consider the case where the array is steered away from a source. In this case, the mean phase error, $\overline{\delta^2}$, is large and the mean sidelobe level is given by

$$\langle \cos^2(\mathbf{s}, \mathbf{d}) \rangle = \overline{L} = \frac{1}{N_e} \tag{42}$$

ADAPTIVE MFB MISMATCH EFFECTS

Assuming a single point source and uniform incoherent noise, the covariance matrix is given by Eq. 10 with $\Lambda = \mathbf{I}$. The adaptive MFB array spectral output degradation due to mismatch—obtained using Eq. 9, A-3, and 38—is given by

$$ASOD_A = 10 \log\left[\frac{\langle E_{A\text{-}MM}\rangle}{\langle E_A\rangle}\right] = -10 \log\left(1 + N\alpha^2\left[1-\cos^2(\mathbf{s},\mathbf{d})\right]\right) \tag{43}$$

$ASOD_A$ is plotted versus mismatch AGD for various output SNRs, $N\alpha^2$, in figure 8. At high output SNRs, large degradation results from rather small mismatch. In this case, the adaptive processor is nulling the portions of the signal that do not match the replica. However, low-level signals near the output noise level (–10 log N) have degradation only slightly larger than the degradation from linear MFB. The adaptive processor does not null the mismatch portions of low-level signals.

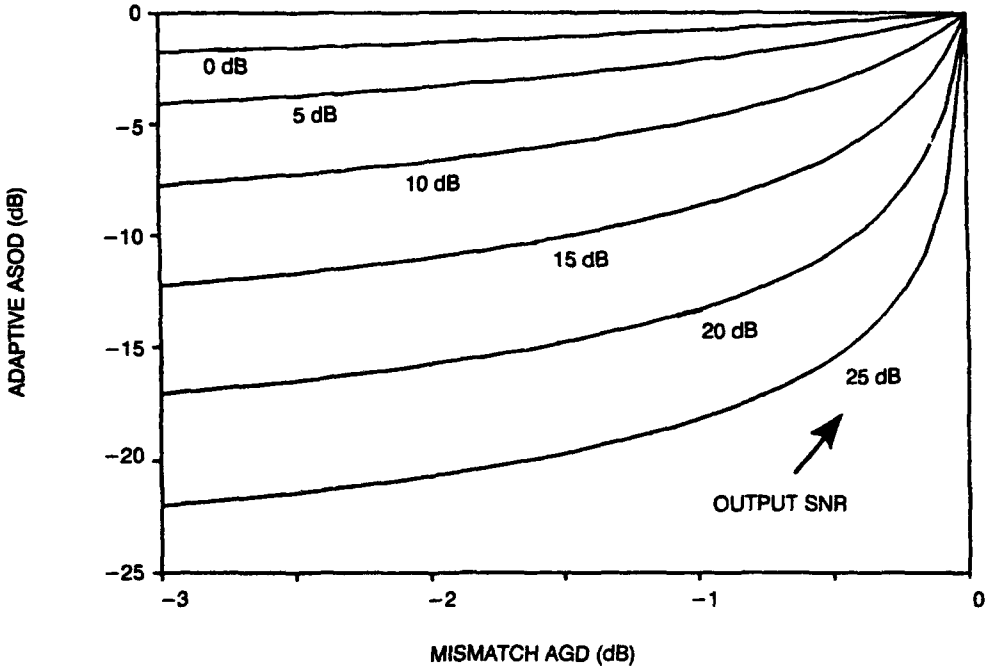

Figure 8. Adaptive array gain degradation versus mismatch array gain degradation for various output SNRs.

Mismatch errors with adaptive MFB thus degrade the performance more than linear MFB only at high SNR. At low output SNR, the mismatch degradation is approximately the same as with linear MFB. The dynamic range of the search space is thus compressed.

The degradation at high SNR can be reduced by bounding the magnitude of the adaptive weight vectors using the white noise constraint algorithm.[13,15,16,17] These methods prevent nulling of the signal in the main beam by limiting the depth of the nulls in the focal pattern. For high-level interferences, the contribution to the noise floor shown in figure 5 will be greater than shown, depending on the value of the bound of the weight magnitude.

CONCLUSIONS

Adaptive matched-field beamforming with large arrays is predicted to achieve gain equal to the directivity index plus the total IINR. An example of a physically derived distribution of received interference levels illustrates that measurements with volumetric arrays of approximately 1,000 hydrophones can determine the IINR, enabling an estimation of achievable array gain.

Array sidelobe level requirements for adaptive MFB are derived, showing that loud interferences contribute less than 1 dB to the noise floor for peak sidelobes below -6 dB re the main lobe. A few sidelobes as high as –3 dB are acceptable.

Adaptive matched-field gain degradation from replica errors is shown to approach the linear matched-field gain degradation at low output SNR.

REFERENCES

1. H. P. Bucker, "Use of calculated sound fields and matched-field detection to locate sound sources in shallow water," J. Acoust. Soc. Am. **59**, 368–373 (1976).
2. M. B. Porter, R. Dicus, and R. G. Fizell, "Simulation of matched-field processing in a deepwater Pacific environment," IEEE J. Ocean. Eng. **OE–12**, 173–181 (1987).
3. R. G. Fizell, "Application of high-resolution processing to range and depth estimation using ambiguity function methods," J. Acoust. Soc. Am. **82**, 606–613 (1987).
4. A. B. Baggeroer, W. A. Kuperman, and H. Schmidt, "Matched field processing: Source localization in correlated noise as an optimum parameter estimation problem," J. Acoust. Soc. Am. **83**, 571–587 (1988).
5. J. S. Perkins and W. A. Kuperman, "Environmental signal processing: Three-dimensional matched-field processing with a vertical array," J. Acoust. Soc. Am. **87**, 1553–1556 (1990).
6. H. Schmidt, A. B. Baggeroer, W. A. Kuperman, and E. K. Scheer, "Environmentally tolerant beamforming for high-resolution matched field processing: Deterministic mismatch," J. Acoust. Soc. Am. **88**, 1851–1862 (1990).
7. W. A. Kuperman, M. D. Collins, J. S. Perkins, and N. R. Davis, "Optimal time-domain beamforming with simulated annealing including application of a priori information," J. Acoust. Soc. Am. **88**, 1851–1862 (1990).
8. N. Owsley, Chapter 3 in *Array Signal Processing*, S. Haykin Ed., Prentice–Hall, Inc. (1985).
9. J. V. Thorn, N. O. Booth, and J. C. Lockwood, "Random and Partially Random Arrays," J. Acoust. Soc. Am. 67, 1277–1286 (1980).
10. J. C. Lockwood, J. V. Thorn, and N. O. Booth, "Directivity index of arrays of random line arrays," J. Acoust. Soc. Am. **72**, 162–180 (1982).
11. _____, "Arrays of random line arrays with constrained element separations," J. Acoust. Soc. Am. **72**, 1474–1477 (1982).
12. B. D. Steinberg, *Principles of Aperture and Array System Design* (Wiley, New York, 1976).

13. H. Cox, "Resolving power and sensitivity to mismatch of optimum array processors," J. Acoust. Soc. Am. **54**, 771–785 (1973).

14. H. G. Berman and A. Berman, "Effect of Correlated Phase Fluctuations on Array Performance," J. Acoust. Soc. Am. **34**, 555–562 (1962).

15. H. Cox, R. M. Zeskind, and M. M. Owen, "Robust Adaptive Beamforming," IEEE Trans. Acoust., Speech, and Signal Proc., **ASSP–35**, 10, p. 1365 (1987).

16. P. M. Velardo, "Robust matched field source localization," Masters thesis, Masachusetts Institute of Technology (1989).

17. M. Reuter, "Characterizing and improving the performance of the MVDR processor," Naval Ocean Systems Center, Technical Document 1983, (November 1990).

Appendix

INVERSE OF $\mathbf{K}_n$

$\mathbf{K}_n$ in Eq. 21 is of the form

$$\mathbf{C}_m = \sum_{j=1}^{m} \mathbf{b}_j \mathbf{d}_j^+ + \mathbf{I} \tag{A-1}$$

where it is assumed that the interferences are orthogonal:

$$\mathbf{b}_j^+ \mathbf{b}_k = b_j^2 \delta_{jk} \tag{A-2}$$

This appendix shows the proof by induction that

$$\mathbf{C}_m^{-1} = \mathbf{I} - \sum_{j=1}^{m} \frac{\mathbf{b}_j \mathbf{b}_j^+}{1 + b_j^2} \tag{A-3}$$

Define

$$\begin{aligned} \mathbf{C}_0 &= \mathbf{I} \\ \mathbf{C}_1 &= \mathbf{C}_0 + \mathbf{b}_1 \mathbf{b}_1^+ \\ \mathbf{C}_2 &= \mathbf{C}_1 + \mathbf{b}_2 \mathbf{b}_2^+ \\ &\vdots \\ \mathbf{C}_m &= \mathbf{C}_{m-1} + \mathbf{b}_m \mathbf{b}_m^+ \end{aligned} \tag{A-4}$$

Eq. 17 can be used to show that

$$\mathbf{C}_k^{-1} = \mathbf{C}_{k-1}^{-1} - \frac{\mathbf{C}_{k-1}^{-1} \mathbf{b}_k \mathbf{b}_k^+ \mathbf{C}_{k-1}^{-1}}{1 + \mathbf{b}_k^+ \mathbf{C}_{k-1}^{-1} \mathbf{b}_k} \tag{A-5}$$

Thus, using Eq. A–2

$$\begin{aligned}
\mathbf{C}_0^{-1} &= \mathbf{I} \\
\mathbf{C}_1^{-1} &= \mathbf{I} + \frac{\mathbf{b}_1 \mathbf{b}_1^+}{1 + b_1^2} \\
\mathbf{C}_2^{-1} &= \mathbf{I} - \frac{\mathbf{b}_1 \mathbf{b}_1^+}{1 + b_1^2} - \frac{\mathbf{b}_2 \mathbf{b}_2^+}{1 + b_2^2} \\
&\vdots
\end{aligned} \tag{A-6}$$

If we assume that

$$\mathbf{C}_{m-1}^{-1} = \mathbf{I} - \sum_{j=1}^{m-1} \frac{\mathbf{b}_j \mathbf{b}_j^+}{1 + b_j^2} \tag{A-7}$$

then, using Eq. A-5

$$\begin{aligned}
\mathbf{C}_m^{-1} = \mathbf{I} &- \sum_{j=1}^{m-1} \frac{\mathbf{b}_j \mathbf{b}_j^+}{1 + b_j^2} \\
&- \frac{\mathbf{b}_m \mathbf{b}_m^+ - \sum_{j=1}^{m-1} \mathbf{b}_j \mathbf{b}_j^+ \mathbf{b}_m \mathbf{b}_m^+ - \sum_{j=1}^{m-1} \mathbf{b}_m \mathbf{b}_m^+ \mathbf{b}_j \mathbf{b}_j^+ + \left[\sum_{j=1}^{m-1} \mathbf{b}_j \mathbf{b}_j^+ \mathbf{b}_m\right] \left[\sum_{j=1}^{m-1} \mathbf{b}_m^+ \mathbf{b}_j \mathbf{b}_j^+\right]}{1 + b_m^2 - \sum_{j=1}^{m-1} \frac{\mathbf{b}_m^+ \mathbf{b}_j \mathbf{b}_j^+ \mathbf{b}_m}{1 + \mathbf{b}_j^2}}
\end{aligned} \tag{A-7}$$

All the sums in the third term are zero by the orthogonality assumption, Eq. A-2, yielding Eq. A-3.

REPORT DOCUMENTATION PAGE

Form Approved
OMB No. 0704-0188

1. AGENCY USE ONLY *(Leave blank)*	2. REPORT DATE	3. REPORT TYPE AND DATES COVERED
	September 1994	Final: Oct 1989 to Oct 1990

4. TITLE AND SUBTITLE
SIGNAL-TO-NOISE GAIN FROM ADAPTIVE MATCHED-FIELD BEAMFORMING OF MULTIDIMENSIONAL ACOUSTIC ARRAYS

5. FUNDING NUMBERS
PE: 0602314N
WU: DN308291
PROJ: RJ14D35
TASK: 730-SW17

6. AUTHOR(S)
Newell O. Booth
Gary L. Mohnkern

7. PERFORMING ORGANIZATION NAME(S) AND ADDRESS(ES)
Naval Command, Control and Ocean Surveillance Center (NCCOSC)
RDT&E Division
San Diego, CA 92152–5001

8. PERFORMING ORGANIZATION REPORT NUMBER
TR 1661

9. SPONSORING/MONITORING AGENCY NAME(S) AND ADDRESS(ES)
Office of Naval Research
800 North Quincy Street
Arlington, VA 22217

10. SPONSORING/MONITORING AGENCY REPORT NUMBER

11. SUPPLEMENTARY NOTES

12a. DISTRIBUTION/AVAILABILITY STATEMENT
Approved for public release; distribution is unlimited.

12b. DISTRIBUTION CODE

13. ABSTRACT *(Maximum 200 words)*

Linear and adaptive matched-field beamforming of multidimensional arrays provide signal-to-noise gain and an estimation of range, depth, and azimuth of the sources of incident signals. Adaptive matched-field beamforming (MFB) with large arrays is predicted to achieve gain equal to the directivity index plus the total input-interference-to-independent-noise ratio (IINR). An example distribution of received interference levels illustrates that measurements with relatively small volumetric arrays can determine the IINR, enabling an estimation of achievable array gain. Array sidelobe level requirements for adaptive MFB are derived, showing that good performance is obtained with relatively high sidelobes. Adaptive matched-field gain degradation from replica errors is shown to approach the linear matched-field gain degradation at low-output-signal-to-noise ratios.

14. SUBJECT TERMS
adaptive array
adaptive interference suppression algorithms
cross-spectral matrix
matched-field beamforming
matched-field processing
minimum variance distortionless response (MVDR)
MVDR beamforming

15. NUMBER OF PAGES
29

16. PRICE CODE

17. SECURITY CLASSIFICATION OF REPORT	18. SECURITY CLASSIFICATION OF THIS PAGE	19. SECURITY CLASSIFICATION OF ABSTRACT	20. LIMITATION OF ABSTRACT
UNCLASSIFIED	UNCLASSIFIED	UNCLASSIFIED	SAME AS REPORT

21a. NAME OF RESPONSIBLE INDIVIDUAL	21b. TELEPHONE *(include Area Code)*	21c. OFFICE SYMBOL
Newell O. Booth	(619) 553–2056	Code 541

INITIAL DISTRIBUTION

Code 0012	Patent Counsel	(1)
Code 0274	Library	(2)
Code 0275	Archive/Stock	(6)
Code 50	H. O. Porter	(1)
Code 54	J. H. Richter	(1)
Code 541	H. P. Bucker	(1)
Code 541	P. A. Baxley	(1)
Code 541	D. Rees	(1)
Code 541	F. J. Ryan	(1)
Code 541	P. W. Schey	(1)
Code 541	B. J. Sotirin	(1)
Code 541	N. O. Booth	(6)
Code 57	R. H. Moore	(1)
Code 702	D. A. Hanna	(1)
Code 705	M. F. Morrison	(1)
Code 71	J. M. Holzmann	(1)
Code 712	D. K. Barbour	(1)
Code 7801	B. Williams	(1)
Code 784	J. C. Lockwood	(1)
Code 807	R. D. Fraser	(3)

Defense Technical Information Center
Alexandria, VA 22304-6145 (4)

NCCOSC Washington Liaison Office
Washington, DC 20363-5100

Center for Naval Analyses
Alexandria, VA 22302-0268

Navy Acquisition, Research and Development
Information Center (NARDIC)
Arlington, VA 22244-5114

GIDEP Operations Center
Corona, CA 91718-8000

Office of Naval Research
Arlington, VA 22217-5000 (3)

Naval Research Laboratory
Washington, DC 20375-5320 (3)

Naval Undersea Warfare Center
Washington, DC 20362-5101 (2)

Space and Naval Warfare Systems Command
2451 Crystal Drive
Arlington, VA 22245-5200 (2)

University of California, San Diego
Marine Physical Laboratory
San Diego, CA 92166-6049